Biferrocene Polymers

Multifunctional Redox Polymers: Electrochrome, Polyelectrolyte, Sensor, Electrode Modifier, Nanoparticle Stabilizer, and Catalyst Template**

Christophe Deraedt, Amalia Rapakousiou, Yanlan Wang, Lionel Salmon, Melanie Bousquet, and Didier Astruc

Dedicated to Alan H. Cowley on the occasion of his 80th birthday

Abstract: *Simple "click" polycondensation metallopolymers of redox-robust bis(ethynyl)biferrocene (biFc) and di(azido) poly(ethylene glycol) (PEG400 and PEG1000) were designed for multiple functions including improvement of water solubility and biocompatibility, the introduction of mixed valency and sensing capabilities, and as nanoparticle stabilizers for catalysis.*

The development of sustainable and biocompatible nanomaterials that have a variety of functions is highly desirable.[1] Here we propose a significant step toward this goal by using biferrocene units to construct water-soluble polymers, which can be used for a variety of applications including sensing and catalysis. Nowadays, a variety of ferrocene-based polymers are known, which exhibit very useful electrochromic properties. For example, orange ferrocene polymers that turn blue upon oxidation to ferricenium were synthesized by ring-opening polymerization of ferrocenophanes by Manners and co-workers.[2] To strengthen the electron-deficient ferricenium groups in polymers, we have now synthesized biferrocene[3,4] polymers in which the electron-releasing ferrocene units stabilize the adjacent ferricenium units to produce robust blue-green mixed-valence biferrocenium polymers. In addition to the electrochromic properties, these new metallopolymers have been constructed with poly(ethylene glycol) (PEG) chains that not only introduce water solubility and biocompatibility to the nanomaterials but also provide reasonable dimesions to make use of the enhanced permeability and retention (EPR) effect to achieve accumulation in cancer cells.[5] The PEG chains and biferrocene (BiFc) units have been assembled by the copper-catalyzed alkyne–azide 1,3-cycloaddition (CuAAC) reaction ("click" chemistry),[6, 7] generating 1,2,3-triazole (trz) linkages. Indeed, these heterocyclic nitrogen ligands are known to sense and stabilize transition-metal ions such as Pd^{II} and Au^{III}, which in turn are precursors for useful metal nanoparticles (NPs) if the polymer can protectively encapsulate and stabilize them.[8] Small Pd NPs and Au NPs are efficient catalysts for a variety of reactions, and their stabilization through the triazole-containing polymer would be a fast and efficient way to provide templated catalysts. Depending on the Au^{III} to Au^0 reduction mode, the size of the Au NPs might be tuned for various applications in catalysis or biomedicine, in which the PEG coating provides additional benefits. Another interesting property of the biferrocene polymers is that the parent unit itself reduces Au^{III} to the polymer-stabilized Au NPs.

The synthesis of the copolymers PEG-trz-biFc **4** [poly-(PEG$_{400}$-biFc)] and **5** [poly(PEG$_{1000}$-biFc)] was achieved by the simple CuAAC "click" reaction between bis-azido-poly(ethylene glycol) with molecular weights of 400 or 1000 g mol^{-1} (PEG$_{400}$ and PEG$_{1000}$; **1** and **2**, respectively)[9] and 1,1'-biethynyl-biFc **3**.[10] The biferrocene unit provides the electrochemical properties (recognition ability, polyelectrolytic and polyelectrochromic features) while the PEG chains of variable length introduce tunable solubility into the polymer. The 1,2,3-triazole ring constructed by "click" chemistry stabilizes active palladium nanoparticles for catalysis of the Suzuki–Miyaura[11] reaction, which was performed with as little as 2 to 20 ppm of Pd. Additionally, gold nanoparticles were used to efficiently catalyze the reduction of 4-nitrophenol.

The "click" polymerization (polycondensation) between **1** or **2** and diethyne **3** is carried out at 40 °C over 2 days in THF/H$_2$O (3:2) using the Sharpless–Fokin catalyst consisting of CuSO$_4$, H$_2$O (5 equiv), and sodium ascorbate (NaAsc; Scheme 1). After removal of the copper ions the polymers are precipitated from Et$_2$O providing **4** as a red-orange air-stable film and **5** as a paste in 78 % and 58 % yield, respectively (see the Supporting Information, SI).

These neutral metallopolymers have been fully characterized by NMR, UV/Vis, and IR spectroscopy, matrix-assisted laser desorption/ionization time-of-flight (MALDI-TOF) mass spectrometry, elemental analysis (EA), cyclic
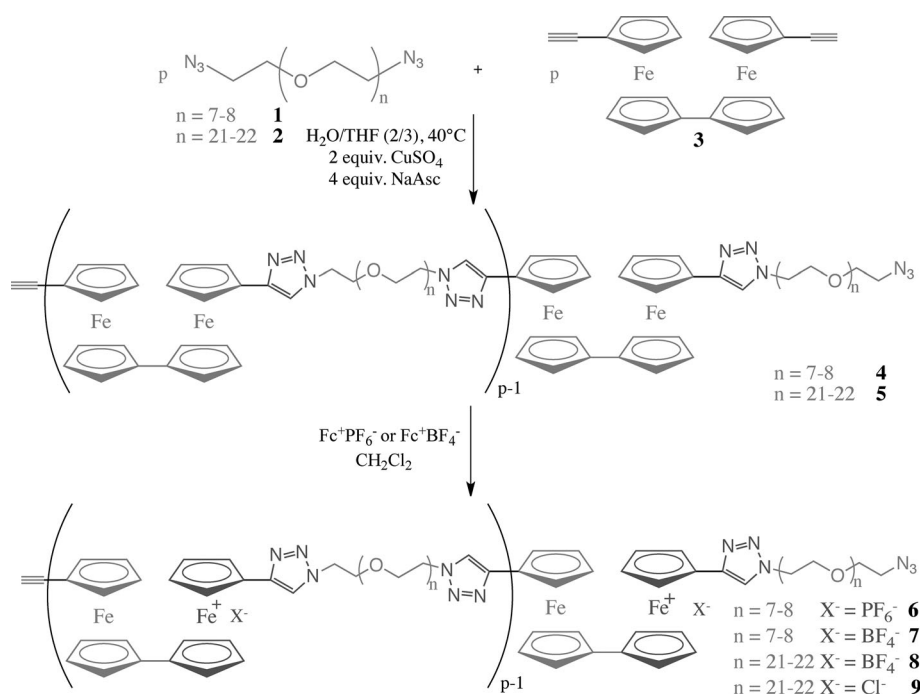
[*] C. Deraedt, A. Rapakousiou, Y. Wang, Prof. D. Astruc
ISM, UMR CNRS N°5255, Univ. Bordeaux
33405 Talence, cedex (France)
E-mail: d.astruc@ism.u-bordeaux.fr
Homepage: http://astruc.didier.free.fr

M. Bousquet
Laboratoire de Chimie des Polymères Organiques
UMR CNRS N° 5629, Univ. Bordeaux
33607 Pessac, cedex (France)

Dr. L. Salmon
Laboratoire de Chimie de Coordination UPR CNRS N°8241
31077 Toulouse cedex (France)

Scheme 1. Synthesis of the PEG-biFc polymers **4** and **5** and the mixed-valence polymers **6–9**).

molecular properties: because of their redox properties and as stable and isolable mixed-valence compounds, they can act as molecular electron storage systems. Cyclic voltammetry involving the bis(trz-Fc) units has been applied to sense ions with potential applications such as the fabrication of modified electrodes. The solubilization properties of the two polymers with distinct PEG lengths are complementary; indeed **4** is soluble only in CH_2Cl_2, $CHCl_3$, DMF, whereas due to the long PEG chain, **5** is soluble in many more solvents including THF, MeOH, EtOH, and H_2O.

The cyclic voltammograms of **4** and **5** measured with a Pt electrode in CH_2Cl_2 using 0.1M $[nBu_4N][PF_6]$ as the supporting electrolyte and decamethylferrocene, $[Cp*_2Fe]$ $(Cp* = \eta^5\text{-}C_5Me_5)$, as the internal reference show two reversible waves at 0.440 and 0.785 V vs. $[Cp*_2Fe]^{+/0}$ (Figure 1 a) and 0.420 and 0.800 V vs. $[Cp*_2Fe]^{+/0}$ (SI), respectively. The presence of only two reversible waves, like in biferrocene itself, implies that the two Fc moieties of one biFc unit are dependent on each other, whereas each biFc unit is independent of other biFc units. One interesting
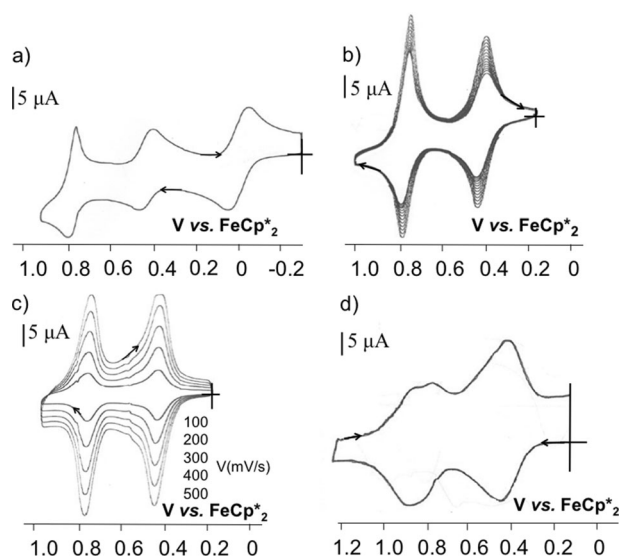
voltammetry (CV), and size-exclusion chromatography (SEC) (SI). Mass spectrometry shows that **4** is composed of at least eight co-units, which corresponds to 15 trz rings. No higher polymer has been observed by mass spectrometry presumably due to saturation of the detector with small oligomers. The polydispersity of PEG_{1000} prevents the observation of **5** by mass spectrometry. No chain terminus ($CH_2\text{-}N_3$ or $\text{-}C\equiv CH$) has been observed in the NMR spectra of either polymer. The polymeric nature of **4** and **5** was also confirmed by IR spectroscopy (no vibrations corresponding to azide and alkyne groups were found) and by CV measurements (estimation for **4**: 62 ± 12 co-units; **5**: 131 ± 20 co-units; SI). The dispersity of the polymers was measured by SEC analyses (**4**: D = 1.24 and **5**: D = 1.27) and is particularly low for a polycondensation process, which makes it possible to exclude the formation of macrocycles. If any macrocycles would be formed in small quantities, they would be removed during the precipitation from ether.[12]

The polymers exhibit a variety of interesting features. First of all, the synthesis is very simple, because only one step is needed from known products, and the CuAAC reaction conveniently yields products, which are easy to purify. Secondly, the use of PEG units introduces biocompatibility, while at the same time the easy availability and simple synthesis from the starting materials **1** and **2** is maintained. Additionally, the use of linear PEG minimizes steric bulk around the trz-biFc-trz units. Thirdly, the "click" chemistry provides triazolyl groups, which are important for the binding of metals and the stabilization of metal NPs. The crucial role of the trz rings in the catalysis by metal NPs is exemplified below.[13] Finally, the presence of biFc units results in multiple stable redox states, which is the most interesting feature of polymers **4** and **5**. These polymers have multifaceted supra-

Figure 1. a) Cylic voltammogram of **4** in CH_2Cl_2; reference electrode: Ag; working and counter electrodes: Pt; scan rate: 0.2 Vs^{-1}; supporting electrolyte: $[nBu_4N][PF_6]$. Two reversible waves are present, one at 0.440 V and a second at 0.785 V. b) Progressive adsorption of **4** upon scanning around the biFc area. c) The modified Pt electrode at various scan rates in a CH_2Cl_2 solution, which only contains the supporting electrolyte). d) Splitting of the second oxidation wave upon addition of $Pd(OAc)_2$ to **4** (1 equiv of Pd^{II} per BiFc unit).

feature of **4** is its progressive adsorption on the electrode, as can be seen from the cyclic voltammogram (Figure 1 b). This allows the facile formation of robust metallopolymer-modified electrodes upon scanning back and forth around the biFc potential zone (Figure 1 c). Variation of the intensity with the scan rate during the electrode modification provides a linear function as it would be expected for a correctly modified electrode (SI). The adsorption of **5** on the electrode is weaker than that of **4** owing to the better solubility of **5** and its ferricenium form. The CV behavior of **4** allows its use and that of the corresponding modified electrode for ion recognition. After addition of Pd(OAc)$_2$ to a solution of **4**, a splitting of 70 mV of the second biFc oxidation wave is observed, reflecting the coordination of Pd^{II} to the nitrogen atoms of the trz ligand. This modifies the electron density of the Fc centers (Figure 1 d). The complexation of Pd(OAc)$_2$ by trz can also be monitored by ^{1}H NMR spectroscopy in CDCl$_3$/MeOH (this solvent mixture was also used in the Pd NP catalysis, see below). The ^{1}H NMR signal of the acetate is shifted upon addition of **4**. This shift is observed until 1 equiv Pd(OAc)$_2$ per triazolyl ring has been added (SI). The 1:1 stoichiometry of Pd^{II}/trz ligand proves to be important in catalysis (see below), when Pd NPs resulting from the reduction of trz-coordinated Pd^{II} species are used.

The proximity of the Fc moieties in the BiFc units implies another application, which is the synthesis of stable mixed-valence polymers affording electrochromic and polyelectrolyte materials. The mixed-valence polymers **6** and **7** were quantitatively synthesized by stoichiometric exergonic reactions of **4** in CH$_2$Cl$_2$ with [Cp$_2$Fe][PF$_6$] and [Cp$_2$Fe][BF$_4$], respectively, because the redox potential of [Cp$_2$Fe]$^{+/0}$ is higher than the first oxidation potential of the biFc$^{+/0}$ units. An additional driving force for these reactions is the precipitation of the mixed-valence polymers **6** and **7** from CH$_2$Cl$_2$. The acetonitrile-soluble polymers **6** and **7** are blue-green, whereas the starting material **4** is orange. Likewise, the mixed-valence polymer **8** was synthesized from **5** in the presence of 1 equiv [Cp$_2$Fe][BF$_4$] per biFc unit and fully characterized (SI). The mixed-valence polyelectrolytes **6** and **7** are insoluble in water, whereas **8** is water-soluble. The three polymers were characterized by UV/Vis, FTIR, near-IR, and Mössbauer spectroscopy. The FTIR spectrum of **6** inconveniently contains a band of PF$_6^-$ at 841 cm^{-1}, but both the ferrocenyl and the ferricinium groups of the BF$_4^-$ polymeric salts **7** and **8** are detected at 818 cm^{-1} (ν_{Fc}) (compare to 819 cm^{-1} in **4**) and 832 cm^{-1} (ν_{Fc*}), respectively (SI), indicating a localized mixed valency even at high IR frequency (10^{13} s^{-1}), which was already observed for the parent biferrocenium. Further proof of this class II mixed valency is the presence of absorption bands in the near-infrared range corresponding to a transition from the ground state to the intervalence charge-transfer (IVCT) state (SI). The recorded Mössbauer spectrum of **6** (Figure 2) at zero field and 78 K further confirms the localized class II mixed valency with the presence of both the ferrocenyl and the ferricinium groups, which was expected since this spectroscopic method covers lower frequencies (10^7 s^{-1}) than IR. Finally in the UV/Vis spectra the λ_{max} of **6–8** (ca. 600 nm) was strongly shifted relative to the λ_{max} of **4** and **5** (ca. 456 nm) (SI).
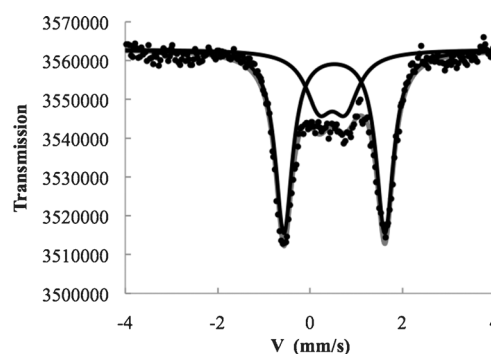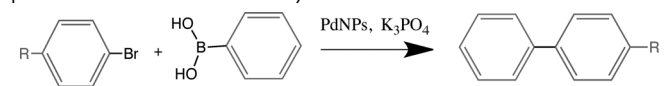

Figure 2. Mössbauer spectrum of **6** at zero field and 78 K showing the localized class II mixed valency at 10^7 s^{-1} with both ferrocenyl (doublet I.S. = 0.536 mm s^{-1} vs. Fe; Q.S. = 2.192 mm s^{-1}) and ferricinium groups (doublet I.S. = 0.490 mm s^{-1} vs. Fe; Q.S. = 0.571 mm s^{-1}).

The presence of triazole units in the polymer chains allows the coordination of 1 equiv Pd^{II} or Au^{III} ions per heterocycle ligand (see above and SI) and further reduction leads to the formation of polymer-stabilized Pd NPs and Au NPs, respectively. These nanomaterials were shown to be active catalysts for various reactions. In addition, it was shown that the longer PEG chains in **5** (PEG$_{1000}$) result in the solubilization of these stabilized NPs in water.

The Suzuki–Miyaura reaction has been conducted in the presence of Pd NPs stabilized by **4** and **5**. Polymer **4** is mixed with Pd(OAc)$_2$ (1 equiv per triazole unit) in CHCl$_3$/MeOH (2/1) and stirred for 5 min. Then NaBH$_4$ (10 equiv per Pd^{II}) is added to the solution, leading to the formation of black Pd NPs. These stable Pd NPs at a loading of 0.25 mol% Pd are efficient in the Suzuki–Miyaura cross-coupling reaction of various bromoarenes with phenylboronic acid (Table 1) in CHCl$_3$/MeOH (2:1) at 90 °C for 16 h. The water-soluble Pd NPs stabilized by **5** are prepared by mixing aqueous solutions of **5** and K$_2$PdCl$_4$ at 20 °C and stirring for 5 min (1/1 Pd/triazole stoichiometry) followed by the quick addition of a NaBH$_4$ solution (10 equiv per Pd^{II}). The yellow solution of Pd^{II}-**5** instantaneously turned orange-brown (SI), confirming the formation of Pd NPs. Transmission electron microscopy (TEM) reveals that the size of Pd NPs stabilized by **5** is (2.3 ± 0.6) nm after they had been stored for one month, which is ideal for efficient catalysis (Figure 3).

The Suzuki–Miyaura reaction has also been performed with this catalyst system, using the "greener" solvent mixture EtOH/H$_2$O (1:1) at 80 °C for 24 h with only 20 ppm of Pd (Pd NPs). The results are summarized in Table 1 and demonstrate the high activity of **5**-Pd NPs. A loading of only 20 ppm Pd is sufficient to obtain good yields using both activated as well as deactivated bromoarenes. Moreover, the amount of Pd can be further reduced. In the case of the coupling of 4-bromoacetophenone and phenylboronic acid at 80 °C only 2 ppm of Pd was necessary to achieve a reaction yield of 82 % after 36 h (TON = 410 000, TOF = 11 400 h^{-1}). The use of such a low amount of catalyst is very rare in the Suzuki–Miyaura reaction, further underlining the interesting properties of the nanomaterial described here. A comparative table (SI) positions **5**-Pd NPs as one of the best catalysts known for the Suzuki–Miyaura reaction.

Table 1: Results of the Suzuki–Miyaura reaction of bromoarenes in the presence of Pd NPs stabilized by **4** and **5**.

$$R-\text{⬡}-Br + \underset{HO}{\overset{HO}{B}}-\text{⬡} \xrightarrow{\text{PdNPs, } K_3PO_4} \text{⬡}-\text{⬡}-R$$

Bromoarene R =	Conditions[a]	Conv. [%][b]	Yield [%][c]	TON [h^{-1}]	TOF [h^{-1}]
H	A (PdNP-**4**)	100	99	396	24.8
CH$_3$	A (PdNP-**4**)	100	97	388	24.3
OCH$_3$	A (PdNP-**4**)	98	97	388	24.3
NO$_2$	A (PdNP-**4**)	100	99	396	24.8
CHO	A (PdNP-**4**)	100	99	396	24.8
COCH$_3$	A (PdNP-**4**)	100	99	396	24.8
H	B (PdNP-**5**)	100	90	45 000	1875
CH$_3$	B (PdNP-**5**)	100	80	40 000	1667
OCH$_3$	B (PdNP-**5**)	100	78	39 000	1625
NO$_2$	B (PdNP-**5**)	100	91	45 500	1896
CHO	B (PdNP-**5**)	100	91	45 500	1896
COCH$_3$	B (PdNP-**5**)	100	99	49 500	2062

[a] Conditions A: the reactions were carried out with 1 mmol of bromoarene, 1.5 mmol of phenylboronic acid, 2 mmol of K$_3$PO$_4$, and 0.25 mol% of Pd NPs stabilized by **4** in 3 mL of CHCl$_3$/MeOH (2:1) for 16 h at 90°C. Conditions B: the reactions were carried out with 1 mmol of bromoarene, 1.5 mmol of phenylboronic acid, 2 mmol of K$_3$PO$_4$, and 0.002 mol% of Pd NPs stabilized by **5** in 6 mL of EtOH/H$_2$O (1:1) for 24 h at 80°C. [b] The conversion was determined by ^{1}H NMR analysis. [c] Yield of isolated product.

Figure 4. a) TEM image of Au NPs synthesized by reduction of Au^{III} with **5**. b) Size distribution of the Au NPs present in the TEM picture (average size of 98 Au NPs: (12 ± 2) nm).
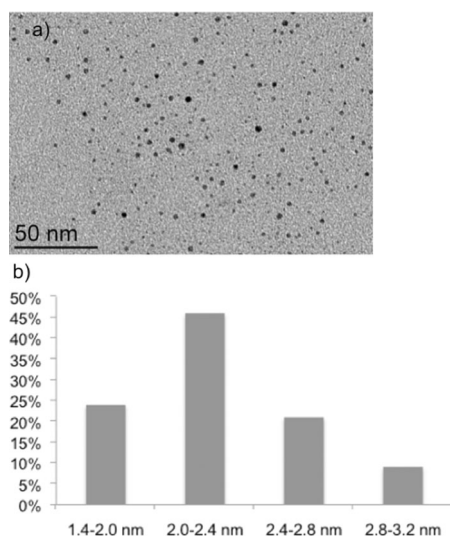

Figure 3. a) TEM image of Pd NPs stabilized by **5**. b) Size distribution of the Pd NPs present in the TEM picture (average size of 103 Pd NPs: (2.3 ± 0.6) nm).

Polymer **5** is oxidized to the mixed-valence water-soluble polyelectrolyte **9** when 1 equiv HAuCl$_4$ is added per 3 equiv biferrocene unit according to the redox stoichiometry, thereby forming Au^0 atoms that give polymer-stabilized Au NPs. Due to the plasmon absorption, which is detected by UV/Vis spectroscopy at 534 nm (SI) the Au NPs solution presents a purple coloration. TEM analysis shows that t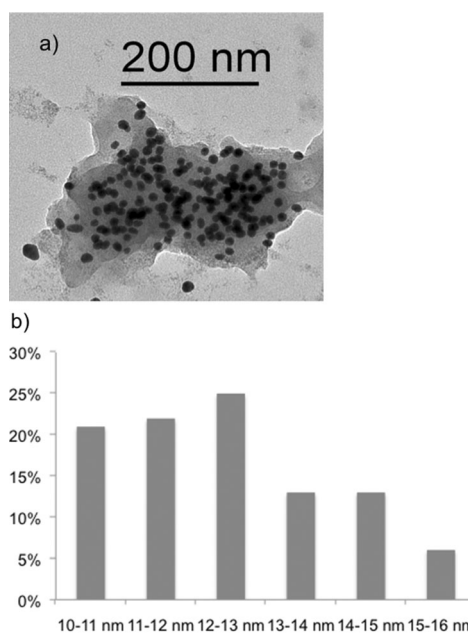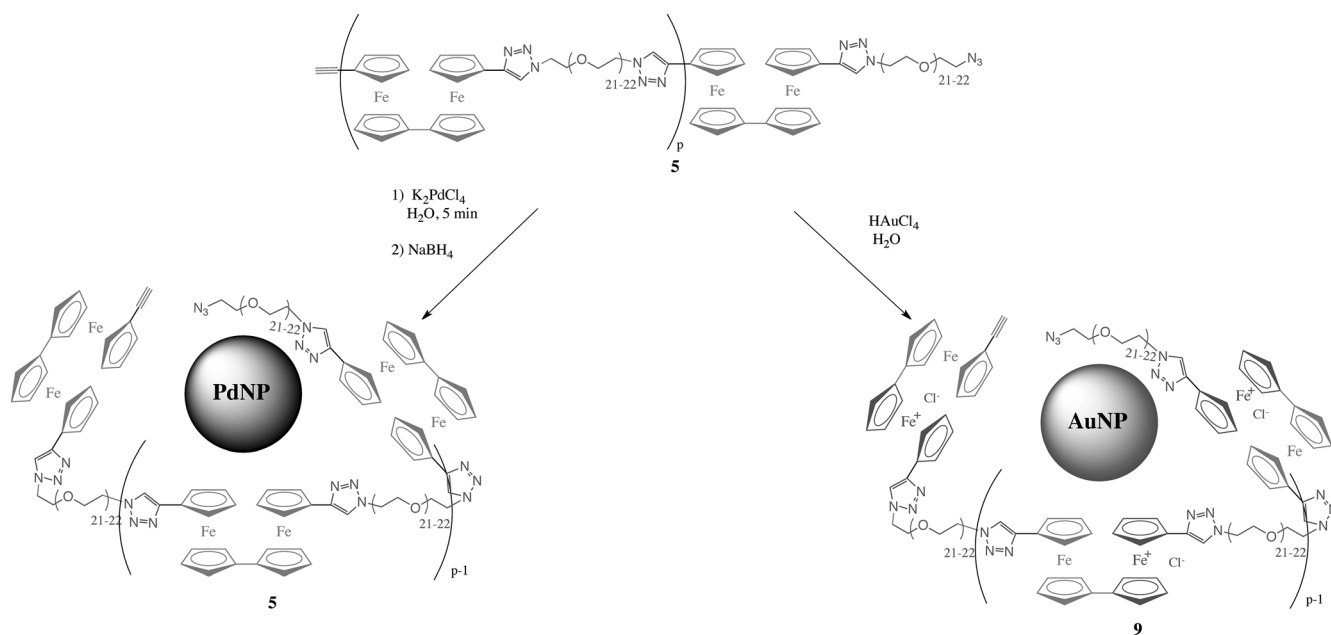hese Au NPs have an average size of around (12 ± 2) nm (Figure 4). Scheme 2 shows the reduction and stabilization of both **5**-PdNPs and **5**-AuNPs. The Au NPs (0.6–1.2 mol%) were used to catalyze the reduction of 4-nitrophenol to 4-aminophenol by an excess of NaBH$_4$; 4-aminophenol is a potential industrial intermediate in the production of many analgesic and antipyretic drugs, anticorrosion lubricants, and hair dyeing agents.[14] When 1.2 mol% of Au NPs is used, the reaction is complete within 350 seconds, which corresponds to a k_{app} value of 6.0×10^{-3} s^{-1}. The reaction rate constant k_{app} is calculated using the rate equation $-\ln(C_t/C_0) = k_{app}t$ (the catalyst exhibits pseudo-first-order kinetics; SI).

In conclusion, the two copolymers **4** and **5** synthesized by "click" polycondensation show multifunctional properties as polyelectrolytes and electrochromes, redox sensors for transition-metal cations, electrode modifiers, and excellent templates for the synthesis of efficient Pd and Au nanoparticle catalysts. The biferrocene unit provides a more stable ferricenium form than the parent ferricenium, which makes the polymers ideal as class II mixed-valence polyelectrolytes and electrochromes. The proximity of the triazole ring to the biFc units facilitates redox sensing as well as the understanding of the stoichiometry of metal cation complexation. The stabilization and solubilization of Pd NPs and Au NPs by easily available polymers yield extremely efficient catalysts for current organic reactions.

Scheme 2. Synthesis of Pd NPs (left) and Au NPs (right).

[1] a) J.-M. Lehn, *Science* **2002**, *295*, 2400–2403; b) J. C. Love, L. A. Estroff, J. K. Kriebel, R. G. Nuzzo, G. M. Whitesides, *Chem. Rev.* **2005**, *105*, 1103–1169; c) M. R. Langille, M. L. Personick, C. A. Mirkin, *Angew. Chem.* **2013**, *125*, 14158–14189; *Angew. Chem. Int. Ed.* **2013**, *52*, 13910–13930; d) D. Astruc, *Nat. Chem.* **2012**, *4*, 255–267.

[2] a) E. M. Leitao, T. Jurca, I. Manners, *Nat. Chem.* **2013**, *5*, 817–829; b) R. Rulkens, A.-J. Lough, I. Manners, S. R. Lovelace, C. Grant, W. E. Geiger, *J. Am. Chem. Soc.* **1996**, *118*, 12683–12695.

[3] a) D. O. Cowan, F. Kaufman, *J. Am. Chem. Soc.* **1970**, *92*, 219–220; b) T. Yamamoto, T. Morikita, T. Maruyama, *Macromolecules* **1997**, *30*, 5390–5396.

[4] a) Y. Men, K. Kubo, M. Kurihara, H. Nishihara, *Phys. Chem. Chem. Phys.* **2001**, *3*, 3427–3430; b) M. Yamada, H. Nishihara, *Chem. Commun.* **2002**, 2578–2579; c) M. Yamada, H. Nishihara, *Eur. Phys. J. D* **2003**, *24*, 257–260; d) C. A. Nijhuis, K. A. Dolatowska, B. Jan Ravoo, J. Huskens, D. N. Reinhoudt, *Chem. Eur. J.* **2007**, *13*, 69–80; e) R. Djeda, A. Rapakousiou, L. Liang, N. Guidolin, J. Ruiz, D. Astruc, *Angew. Chem.* **2010**, *122*, 8328–8332; *Angew. Chem. Int. Ed.* **2010**, *49*, 8152–8156.

[5] a) I. Brigger, C. Dubernet, P. Couvreur, *Adv. Drug Delivery Rev.* **2002**, *54*, 631–651; b) A. Llevot, D. Astruc, *Chem. Soc. Rev.* **2012**, *41*, 242–257.

[6] a) V. V. Rostovtsev, L. G. Green, V. V. Fokin, K. B. Sharpless, *Angew. Chem.* **2002**, *114*, 2708–2711; *Angew. Chem. Int. Ed.* **2002**, *41*, 2596–2599; b) C. W. Tornøe, C. Christensen, M. Meldal, *J. Org. Chem.* **2002**, *67*, 3057–3064.

[7] a) For CuAAC "click" polymer assemblies, see: G. W. Goodall, W. Hayes, *Chem. Soc. Rev.* **2006**, *35*, 280–312; b) M. Malkoch, R. Vestberg, N. Gupta, L. Mespouille, P. Dubois, A. F. Mason, J. L. Hedrick, Q. Liao, C. W. Frank, K. Kingsbury, C. J. Hawker, *Chem. Commun.* **2006**, 2774–2776; c) J. E. Moses, A. D. Moorhouse, *Chem. Soc. Rev.* **2007**, *36*, 1249–1262; d) P. L. Golas, K. Matyjaszewski, *Chem. Soc. Rev.* **2010**, *39*, 1338–1354; e) L. Liang, D. Astruc, *Coord. Chem. Rev.* **2011**, *255*, 2933–2945; f) F. Herbst, S. Seiffert, W. H. Binder, *Polym. Chem.* **2012**, *3*, 3084–3092; g) M. H. Samiullah, D. Reichert, T. Zinkevich, J. Kressler, *Macromolecules* **2013**, *46*, 6922–6935.

[8] a) C. Ornelas, J. Ruiz, E. Cloutet, S. Alves, D. Astruc, *Angew. Chem.* **2007**, *119*, 890–895; *Angew. Chem. Int. Ed.* **2007**, *46*, 872–877; b) A. K. Diallo, C. Ornelas, L. Salmon, J. Ruiz, D. Astruc, *Angew. Chem.* **2007**, *119*, 8798–8802; *Angew. Chem. Int. Ed.* **2007**, *46*, 8644–8648; c) E. Boisselier, A. K. Diallo, L. Salmon, C. Ornelas, J. Ruiz, D. Astruc, *J. Am. Chem. Soc.* **2010**, *132*, 2729–2742.

[9] PEG derivatives **1** and **2** were synthesized from PEG$_{400}$ and PEG$_{1000}$: L. A. Canalle, S. S. van Berkel, L. T. de Haan, J. C. M. van Hest, *Adv. Funct. Mater.* **2009**, *19*, 3464–3470.

[10] Diethynyl biFc **3** was synthesized from ferrocene: T.-Y. Dong, S.-W. Chang, S.-F. Lin, M.-C. Lin, Y.-S. Wen, L. Lee, *Organometallics* **2006**, *25*, 2018–2024.

[11] a) N. Miyaura, A. Suzuki, *Chem. Rev.* **1995**, *95*, 2457–2483; b) J. Hassan, M. Sévignon, C. Gozzi, E. Schulz, M. Lemaire, *Chem. Rev.* **2002**, *102*, 1359–1469; c) F. Bellina, A. Carpita, R. Rossi, *Synthesis* **2004**, 2419–2440; d) I. Beletskaya, A. V. Cheprakov, *J. Organomet. Chem.* **2004**, *689*, 4055–4082; e) D. Astruc, F. Lu, J. Ruiz, *Angew. Chem.* **2005**, *117*, 8062–8083; *Angew. Chem. Int. Ed.* **2005**, *44*, 7852–7872; f) D. Astruc, K. Heuzé, S. Gatard, D. Méry, S. Nlate, L. Plault, *Adv. Synth. Catal.* **2005**, *347*, 329–338; g) I. Favier, D. Madec, E. Teuma, M. Gomez, *Curr. Org. Chem.* **2011**, *15*, 3127–3174; h) *Nanomaterials in Catalysis* (Eds.: P. Serp, K. Philippot), Wiley-VCH, Weinheim, **2013**.

[12] B. P. Mudraboyina, M. M. Obadia, R. Sood, A. Serghei, E. Drockenmüller, *Chem. Mater.* **2014**, *26*, 1720–1726.

[13] a) C. Deraedt, L. Salmon, J. Ruiz, D. Astruc, *Adv. Synth. Catal.* **2013**, *355*, 2992–3001; b) C. Deraedt, D. Astruc, *Acc. Chem. Res.* **2014**, *47*, 494–503.

[14] a) K. Kuroda, M. Haruta, *J. Mol. Catal. A* **2009**, *298*, 7–11; b) S. Wunder, Y. Lu, M. Albrecht, M. Ballauf, *ACS Catal.* **2011**, *1*, 908–916; c) J. P. Zhang, C. Shao, Z. Zhang, M. Zhang, J. Mu, Z. Guo, Y. Liu, *Nanoscale* **2011**, *3*, 3357–3363; d) P. Hervés, M. Pérez-Lorenzo, L. M. Liz-Marzán, J. Dzubiella, M. Ballauf, *Chem. Soc. Rev.* **2012**, *41*, 5577–5587; e) A. Shivhare, S. J. Ambrose, H. Zhang, R. W. Purves, R. W. Scott, *Chem. Commun.* **2013**, *49*, 276–278.